

Scoping Calculations for a Booster on the RAL SNS

D.J. Picton and T.D. Beynon

A series of preliminary scoping calculations has been performed for two alternative strategies for an upgrade to the SNS at the Rutherford Appleton Laboratory. The first strategy would involve the replacement of the present depleted uranium target with an enriched target of similar dimensions. The second strategy involves the design of a separate booster target which would run in parallel with the present target.

The results give information on the following issues: the relative merits of uranium and plutonium systems, the relationship between enrichment and  $k_{eff}$ , and the optimization of decouplers and reflectors.

## 1. INTRODUCTION

The present SNS target has a design power of 230 kW, corresponding to a neutron production rate of  $2.3 \times 10^{16}$  n/s from a proton beam intensity of  $8.7 \times 10^{14}$  p/s. Undoubtedly it is already one of the most powerful neutron sources available to experimentalists, and the concept of a booster system, to provide substantially higher neutron intensities, requires careful justification.

The main priority in upgrading the SNS in future years will probably involve improvements at energies at which its performance is poor compared with reactor sources. Undoubtedly the main area for improvement is in the cold neutron range below 25 meV, particularly the sub 4 meV range. There are two reasons why the SNS fails to match the performance of reactor sources in this area. Pulsed sources are inherently weak at thermal energies, although their epithermal fluxes are relatively large. The second deficiency is due to the fact that the cold source moderator is "downstream" in its position relative to the SNS target, with a subsequent reduction of the neutron flux incident on the cold moderator due to the attenuation of the proton beam.

The booster project falls into two main areas of study. The first, described in this paper, involves the design of improved targets. The second area will involve the optimization of the moderator.

## 2. ENRICHED TARGET CALCULATIONS

### 2.1 General discussion

Two possible strategies for the improvement of the SNS target are described in this paper. This section concentrates on a relatively

unambitious but cheap option, namely the use of a enriched uranium target in place of the present depleted uranium target.

Fig. 1 shows the design of the target station. The target consists of a series of zircalloy-clad uranium plates of varying thickness, cooled by  $D_2O$ . Note how the plate thickness increases in inverse proportion to power density.

Fig. 2 shows the arrangement of the moderator chambers on the SNS target. As previously mentioned, the downstream moderators are cold moderators (liquid  $H_2$  and methane.) The most effective design for an enriched target for the improvement of the cold moderators would involve a varying enrichment, increasing in the downstream direction. A uniform power loading throughout the target would be an ideal to aim for.

At this stage, however, we have concentrated on a series of simple scoping calculations to evaluate the overall performance of a uniformly enriched target.

## 2.2 Computational Details

The geometry and material used in our calculations is based on a benchmark calculation whose original purpose was code comparison. It has a number of unrealistic features; the uranium density in the target is too high, the geometry is over-simplified, and the target is too well-reflected. Nevertheless, the calculations presented here provide a reasonable semi-quantative estimate of target performance as a function of enrichment.

Fig. 3 shows the enriched target geometry, and Table 1 summarizes the atom number densities used. The system consists of a cylindrical target void in line with a cylindrical target, both of diameter 4.5 cm. Both these regions are decoupled with a 1 cm layer of  $^{10}\text{B}$  to prevent the degradation of the fast pulse time distribution via the multiplication of thermal neutrons.

The target and void regions are in turn surrounded by a reflector in the form of a 70 cm cube, containing a mixture of Be and  $\text{D}_2\text{O}$ . The target is  $\text{D}_2\text{O}$  cooled uranium, and the decoupler is  $^{10}\text{B}$ .

Two sets of results are presented. The first relates to target performance as a function of enrichment. The second set of calculations involves the optimization of the decoupler density. The calculations presented in this section were performed by the Monte Carlo code Morse-H (1) using the coupled neutron-gamma library DLC37F (2). The fixed source used in these calculations was the result of modelling using the HETC code (3) for spallation neutron production in the SNS target.

### 2.3 Results

Table 2 presents the results for target performance as a function of  $^{235}\text{U}$  enrichment. The quantities calculated in the table are as follows. The multiplication factor  $M$  is the ratio of total to primary neutron production. The outgoing current represents the total leakage (over all energy groups) in the outgoing direction and the net current is defined as the (outgoing-incoming) leakage. Rough estimates of target power are also given.

For a 65% enriched system, the enrichment gain (i.e. the ratio of enriched to depleted uranium target performance) has a value of 4.6 for the net leakage at the decoupler-reflector interface. It should be noted that the numerical value of the enrichment gain is not very sensitive to the exact performance indicator used; for example the enrichment gain for outgoing leakage is 4.3 in the above case. This estimate certainly exaggerates the performance of a real target, for the reasons given earlier, ie. the density of fissile material would be lower than used here (and would in fact have to decrease with increasing reactivity to permit effective cooling.) A real system will also be less well reflected in the sense that the reflector will contain voids and will not be in intimate contact with the target.

Table 3 presents the results for the decoupler optimization calculations for the 65% enriched system. Here the  $^{10}\text{B}$  density in the decoupler was progressively reduced without changing any other parameter. The main indicator of interest here was the ratio of inward leakage in the thermal group to primary neutron production. At a decoupler density of  $0.00125 \text{ atoms}/(10^{-24} \text{ cm}^3)$  this ratio was about 3%. This unwanted leakage of thermal neutrons into the target would be multiplied and would clearly have an adverse effect on the time distribution of the fast neutron pulse. A firm decision on the decoupler characteristics must await a time-dependent calculation, which has not yet been performed.

### 3. SIMPLE SCOPING CALCULATIONS FOR A BOOSTER SYSTEM.

#### 3.1 General discussion

A second set of scoping calculations was oriented towards a more elaborate option than that described in the previous section. This alternative strategy would involve a second more specialized booster target which would run in parallel with the existing SNS target.

The optimum performance characteristics of a pulsed booster differ considerably from a fast reactor in a number of ways. The neutron leakage at the surface of the booster, and its time distribution, are more relevant performance indicators than total power production. The total neutron multiplication  $M$ , defined as in the previous section, is not given by

$$M_0 = \frac{1}{1-k_{eff}}$$

In most cases  $M$  is larger than  $M_0$  because the first few neutron generations are concentrated towards the centre of the booster, and are therefore relatively unaffected by leakage.

Three basic types of booster system were investigated. A simple but rather unpromising option involves a depleted uranium target surrounded by enriched fuel. A second option involves uniformly enriched fuel. The third arises from the observation above concerning  $M > \frac{1}{1-k_{eff}}$ . In general a system in which enrichment is concentrated in a central region will certainly produce a greater power production, for a given value of  $k_{eff}$ , than a uniformly enriched system. This provides a relatively safe means of increasing power production without a potentially risky increase in  $k_{eff}$  although, of course, surface leakage rather than power production is the main performance indicator for a booster.

### 3.2 Computational Details

All the calculations described in this section were performed using the one dimensional neutron transport code ANISN. In all cases, spherical geometry was employed.

Table 4 summarizes the characteristics of the four models described in this section. All the systems under consideration were based on the concept of a  $^{235}\text{U}$  or  $^{239}\text{Pu}$ -enriched core, surrounded by a 12 cm-thick Ni reflector. No decoupler was specified because nickel does not produce significant thermalization. The net leakage at the core/reflector boundary was used as the main performance indicator for the system. Both integrated intensity and intensity per unit area ("brightness") were evaluated. In all cases the coolant used was sodium uniformly distributed in the core and occupying a volume fraction of 20%.

Model 1 is based on the concept of a highly enriched fissile blanket around a depleted uranium spallation target of similar size to the current SNS target. Model 2 represents the simple case of a uniformly enriched target, and Model 3 represents an attempt to improve performance without increasing  $k_{\text{eff}}$ , by enhancing the multiplication of the first few neutron generations. An inner area of radius 5 cm was given a higher enrichment.

Models 1-3 are based on current oxide fuel technology ( $\text{UO}_2$  or mixed  $\text{PuO}_2/\text{UO}_2$ ). However, the use of a uranium alloy (e.g. uranium molybdenum) would in fact be more appropriate for a spallation target. There are two reasons for this; uranium or plutonium oxides contain about half the concentration of metal atoms compared with the parent metal, and the

presence of a large concentration of oxygen in a spallation target would considerably reduce the neutron yield. Model 4 is similar to Model 2 but based on the more realistic concept of uranium or uranium/plutonium metal alloys. In view of the poor characteristics displayed by models 1 and 3, calculations in these geometrics were not repeated using uranium/plutonium metal fuels.

Two basic types of calculation were performed for each case. In the concentration search calculations, the enrichment required to produce a specified value of  $k_{eff}$  was determined. In the fixed source calculations, a uniformly distributed fixed source was specified in a central region of radius 5 cm. A  $^{235}\text{U}$  fission source was used for the energy distribution.

### 3.3 Results

Fig. 4 shows the results of the concentration search calculation for Models 1-3. In the case of Model 2, there are two sets of curves for both plutonium-enriched and uranium-enriched systems (ie.  $^{238}\text{U}$  enriched with  $^{239}\text{Pu}$  or  $^{235}\text{U}$ ). For models 1 and 3, the results are all for plutonium-enriched systems.

The immediate conclusion which can be drawn in comparing configurations 1 and 2 is that a uniformly enriched system can be considerably more compact than a system containing a depleted uranium core. The difference between the plutonium and uranium systems is as expected from the large difference in critical mass between  $^{235}\text{U}$  and  $^{239}\text{Pu}$ . At a given enrichment, a uranium system needs about 1.5 times the radius of a plutonium-enriched system to produce the same value of  $k_{eff}$ .



Figs 5 to 7 display the results of the fixed source calculations for Models 1-3. Three quantities are presented - integrated net leakage at the core-reflector boundary, net leakage per unit surface area ("brightness") and multiplication factor M (total neutron production per primary source neutron).

One important factor is evident when the curve for integrated leakage is examined. The leakage is a strong function of  $k_{eff}$ , but almost independent of radius when  $k_{eff}$  is kept constant. It is clear that the inhomogeneous enrichment of Model 3 does not produce a substantial improvement in surface leakage. This is in contrast to the results for neutron multiplication, which demonstrate considerably enhanced power production for Model 3.

For most purposes the "brightness" of the source is more important than integrated leakage. The most important factor in determining brightness is the  $\frac{1}{r^2}$  geometric attenuation term. From this point of view it is clear that a system must be reasonably compact in order to provide a bright source for a moderator; Model 1 can be eliminated for this reason.

Fig. 8 to 10 present results for Model 4. Two sets of curves are presented, for  $^{235}\text{U} + ^{238}\text{U}$  fuel and  $^{239}\text{Pu} + ^{238}\text{U}$  fuel.

It is clear from these results that uranium/plutonium metal systems are greatly superior to oxide systems, from a neutronic point of view in addition to the consideration of spallation yield described earlier. Both the uranium and plutonium enriched systems can be substantially more compact than the corresponding  $\text{UO}_2$  and mixed  $\text{PuO}_2 - \text{UO}_2$  systems in Model

2. From this point of view, the use of plutonium (with its environmental disadvantages) can be avoided if necessary. This can be seen by comparing figs 4 and 8 for the oxide and all-metal system, respectively. At  $k_{eff} = 0.9$ , the minimum radius for the uranium oxide system (fig 4, configuration 2) is approximately 9.5 cm compared with a value of about 6 cm for the uranium metal system (fig. 8). The  $PuO_2$  system (fig 4) would achieve the value  $k_{eff} = 0.9$  at a minimum radius of about 6 cm, and would therefore offer no significant advantages over the uranium metal system. Plutonium metal systems cannot be considered as technologically feasible.

#### 4. FURTHER CALCULATIONS FOR ENRICHED TARGET SYSTEMS.

##### 4.1 General discussion

The calculations presented in the previous two sections were mainly concerned with a few fundamental aspects of booster or enriched target design, i.e. the relationships between size, enrichment and overall neutronic performance. The calculations in this section, however, are concerned with more detailed questions about the choice of materials for the target coolant and reflectors.

In the case of coolant material, the effect of substituting sodium for  $D_2O$  was investigated. In addition, the effect of substituting nickel for beryllium as the reflector material was calculated. A somewhat unrealistic nickel reflector, i.e. without coolant or decoupler, was specified in order to evaluate the maximum possible gain in comparison with a more realistic  $D_2O$  cooled Be reflector.

A second question which has been addressed concerned the effect of a reflector whose surface is further from the target. A calculation was performed for a system containing a 1 cm void between the target decoupler

and reflector.

#### 4.2 Computational Details

The geometry used here was based on the modified benchmark geometry in Fig. 3. However, a more realistic composition was assumed for the target, i.e. a homogeneous mixture of uranium (80% volume fraction) and coolant (20% volume fraction).

The two alternative coolant materials used here were sodium and D<sub>2</sub>O. For the reflector material, the alternatives were: D<sub>2</sub>O cooled beryllium (composition as in section 2, Table 1) or nickel. As in section 2, the beryllium reflected targets were surrounded by a 1 cm thick <sup>10</sup>B decoupler (density 10<sup>22</sup> atoms cm<sup>-3</sup>). In addition, a case without a decoupler was run for comparison purposes. In the Ni reflected systems, the decoupler material was omitted; a void region was specified in place of the <sup>10</sup>B.

In section 2, it was found that the multiplication factor M for systems in the enriched target geometry is always close to

$$\frac{1}{1-k_{\text{eff}}}$$

This is not unexpected in view of the small size of the target cylinder in two out of three dimensions. For this reason, a decision was made to maximise computational efficiency by running only  $k_{\text{eff}}$  calculations for all cases. In general, the cost of fixed source calculation is proportional to M (and becomes infinite at  $k_{\text{eff}} > 1$ ). In contrast, the cost of  $k_{\text{eff}}$  calculations is almost independent of reactivity.

### 4.3 Results and Discussion

In table 5, the results of the calculation performed for this section are summarized. In addition, selected results are plotted in Fig. 11.

In the case of the heavy water cooled systems plotted in Fig. 11, the substitution of Ni for Be as the reflector material had a significant positive effect on reactivity. However, the difference seen here represents an upper limit. In practice, the Ni reflector would need to be cooled, probably by D<sub>2</sub>O. The effect of this would be to soften the reflected spectrum, making it more similar to that of the D<sub>2</sub>O cooled Be reflector. In addition, the <sup>10</sup>B decoupler density used for the Be reflected systems was probably unnecessarily high. The results presented in Table 3 suggest that the use of an optimized decoupler with a lower density may increase  $k_{eff}$  by up to 5%, i.e. enough to match the performance of the Ni reflector.

In the case of the sodium cooled systems, the nickel reflector shows a smaller advantage over Be of the order of 1%. The differences between the sodium and heavy water cooled system are probably attributable to the detailed effects of D<sub>2</sub>O moderation on the energy spectrum in the target. The presence of (n,2n) multiplication reactions in beryllium must be taken into account when comparing it with other reflector materials.

### 5. GENERAL CONCLUSIONS

The calculations presented in this paper provide a considerable amount of information on design concepts for an enriched target or booster for a spallation source.

The results in Sections 1 and 3 provide useful estimates of the necessary degree of enrichment required for an enriched target system of similar dimensions to the existing SNS target. In addition, these results provide useful information on reflectors and decouplers. The  $^{10}\text{B}$  decoupler used in most of these calculations appears to have a considerably higher decoupling energy than necessary, although a firm choice of decoupler must await time-dependent calculations. The use of a nickel reflector in place of beryllium appears to present only a marginal advantage. In the case of the coolant material, the use of sodium rather than heavy water carries only a small penalty in reactivity. However, care must be taken in interpreting these results, in the sense that moderators have not been included in the calculations. Any hardening of the spectrum will degrade moderator performance.

In section 2, more basic questions concerning the size, enrichment and choice of fuel for a booster system were answered. A comparison was made between oxide and metal fuels, and between  $^{235}\text{U}$  and  $^{239}\text{Pu}$  enriched systems. The main conclusion to be drawn is that a uranium metal fuel enriched in  $^{235}\text{U}$  is comparable in neutronic performance to a  $^{239}\text{PuO}_2$  enriched  $^{238}\text{UO}_2$  system, and would show a large advantage in spallation efficiency. In the absence of a Pu metal fuel technology, the uranium metal system is clearly the only practical option.

#### References

1. W.W. Engle Jr. Oak Ridge National Laboratory Report No. K1693 (1967).
2. Emmet M.B. The MORSE Monte-Carlo Radiation Transport Code System. Oak Ridge National Laboratory Report ORNL-4972 (1975).
3. T.A. Broome, Rutherford Appleton Laboratory. Private Communication.
4. A.D. Taylor, "Neutron Transport from Targets to Moderators". Meeting on Targets for Neutron Beam Spallation Sources, Jülich, 11-12 June 1979. See also Rutherford Appleton Laboratory Report RL 81 057.

TABLE 1

Particle Number Densities (Atoms/Barn CM)

ZONE	DENSITY
<b>TARGET</b>	
U-238	0.0166 ) ) 65% enriched case
U-235	0.0308 )
D	0.0093
O	0.0047
<b>DECOUPLER</b>	
B-10	0.01
<b>REFLECTOR</b>	
BE	0.0989
D	0.0134
O	0.00669

TABLE 2

Summary of results for the modified benchmark target (Results are normalized to 1.0 primary source neutron).

Enrichment	0	20	40	65
k eff	0.147	0.455	0.662	0.856
Fission source	0.30	0.98	2.15	6.39
Total source	1.30	1.98	3.15	7.39
Outgoing Current:				
Targ. -Dec.	1.48	2.05	2.97	6.44
Dec. -ref.	1.53	2.12	3.09	6.71
Net leakage:				
Targ. -Dec.	0.910	1.25	1.81	3.89
Dec. -ref.	0.532	0.748	1.11	2.43
Power (MeV)	74	132	228	580
<u>Power</u> net leakage (Dec. -ref.)	139	176	204	238

TABLE 3

Decoupler optimization for the 65% enriched modified benchmark

B atom density (per $10^{-24}$ cm <sup>2</sup> )	0.01	0.005	0.0025	0.00125
Total source	7.39	8.19	9.50	11.36
Outgoing current:				
Targ. - Dec.	6.438	7.22	8.44	10.17
Dec. - Refl.	6.708	7.67	9.04	10.98
Net leakage:				
Targ.-Dec.	3.892	4.212	4.756	5.551
Dec.-Refl.	2.437	2.779	3.276	3.964
Ingoing current (thermal group only):				
Dec.-Targ.	0.0	4.0E-5	1.0E-3	3.1E-2

**TABLE 4**

**Booster Model Characteristics.**

Model	Zone 1	Zone 2	Zone 3
1	<p>Radius 7.81 cm</p> <p>80% <math>^{235}\text{U}</math> 20% Na</p>	<p>Variable thickness</p> <p>80% fuel 20% Na Fuel: <math>^{239}\text{PuO}_2</math> + <math>^{238}\text{UO}_2</math></p>	<p>Thickness 12 cm</p> <p>Ni</p>
2	<p>Variable radius</p> <p>80% fuel 20% Na Fuel: <math>^{239}\text{PuO}_2</math> + <math>^{238}\text{UO}_2</math> or <math>^{235}\text{UO}_2</math> + <math>^{238}\text{UO}_2</math></p>	<p>Thickness 12 cm</p> <p>Ni</p>	-
3	<p>Radius 5 cm</p> <p>80% fuel 20% Na Fuel: <math>^{239}\text{PuO}_2</math> + <math>^{238}\text{UO}_2</math></p>	<p>Variable thickness</p> <p>80% fuel 20% Na Fuel: <math>^{239}\text{PuO}_2</math> + <math>^{238}\text{UO}_2</math> (different enrichment)</p>	<p>Thickness 12 cm</p> <p>Ni</p>
4	<p>Variable radius</p> <p>80% fuel 20% Na Fuel: <math>^{239}\text{Pu} + ^{238}\text{U}</math> or <math>^{235}\text{U} + ^{238}\text{U}</math></p>	<p>Thickness 12 cm</p> <p>Ni</p>	-



**TABLE 5**

Further results for the enriched target configurations.

Enrichment	Coolant	Decoupler	Reflector	$k_{eff}$
0	D <sub>2</sub> O	<sup>10</sup> B	Be	0.126±.001
20				0.384±.002
40				0.570±.002
65				0.739±.003
0	D <sub>2</sub> O	void	Be	0.128±.003
10				0.610±.006
20				0.718±.006
40				0.889±.007
65				1.045±.007
0	D <sub>2</sub> O	void	Ni	0.124±.002
20				0.409±.004
40				0.611±.005
65				0.786±.005
0	Na	<sup>10</sup> B	Be	0.723±.005
65				0.130±.002
0	Na	void	Ni	0.1360±.0015
65				0.734±.006
0	D <sub>2</sub> O	void	void	0.123±.002
65				0.511±.004
0	D <sub>2</sub> O	<sup>10</sup> B*	Be	0.1263±.0015
65				0.721±.004

\* surrounded by an additional void region, thickness 1 cm.

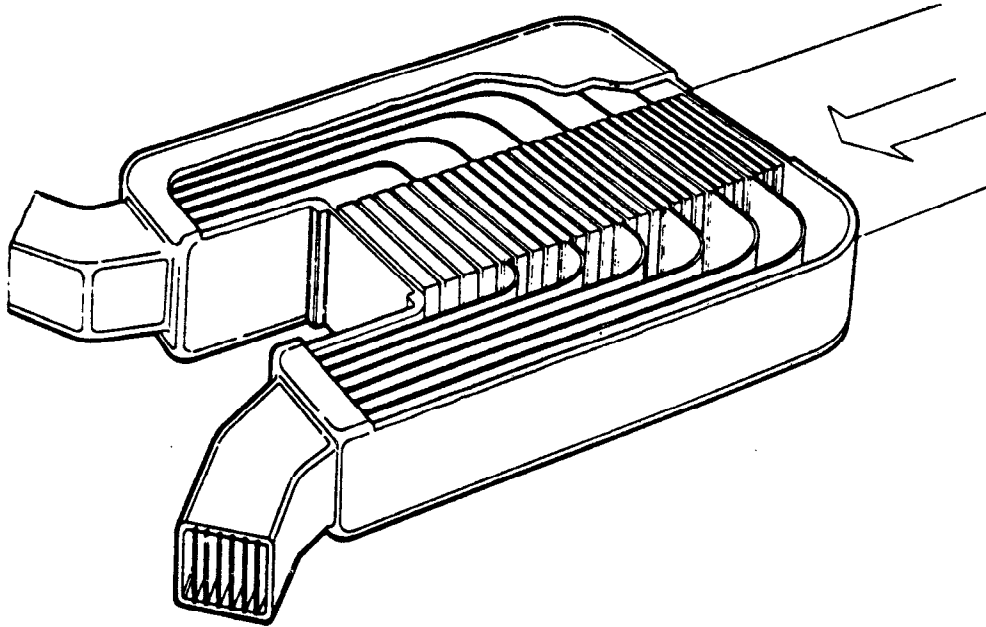


Fig. 1

The high power (200  $\mu$ A) target for SNS at the Rutherford Laboratory <sup>(4)</sup>

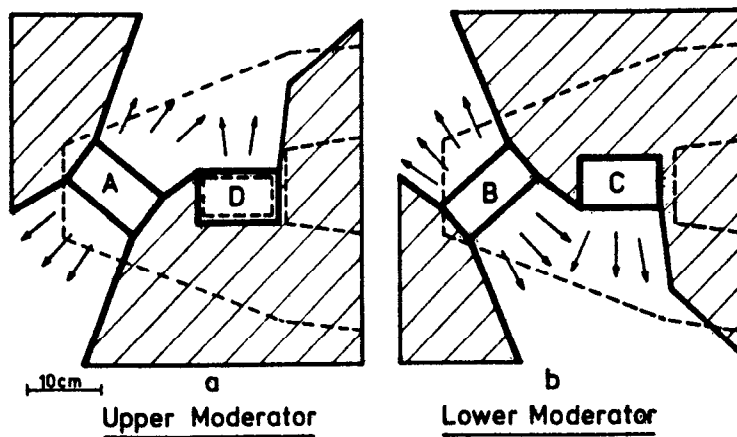


Fig. 2

Schematic representation of the arrangement of the SNS moderators <sup>(4)</sup> relative to the target.

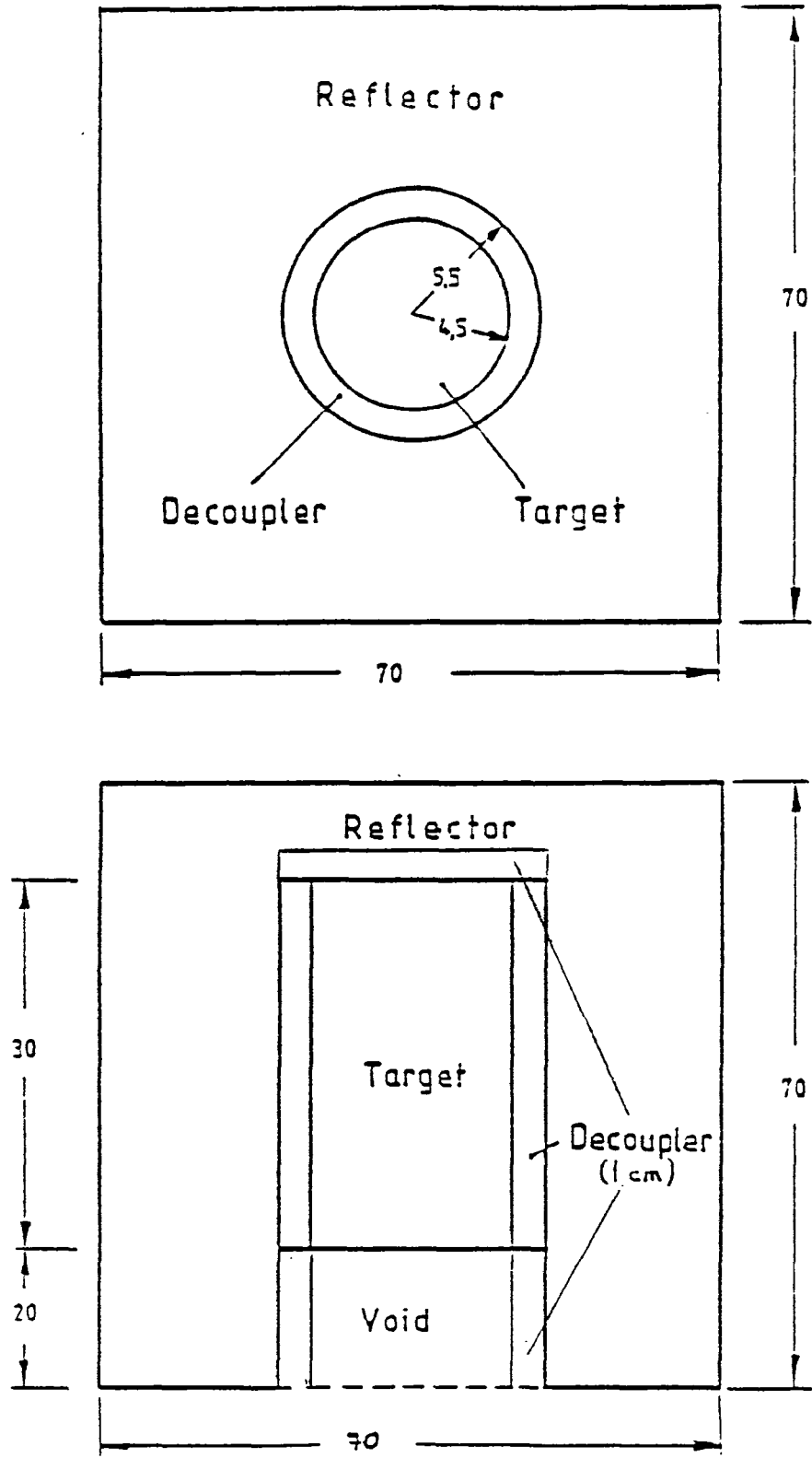


Fig. 3  
 Model for Transport Calculations (modified)  
 (Dimensions in cm)

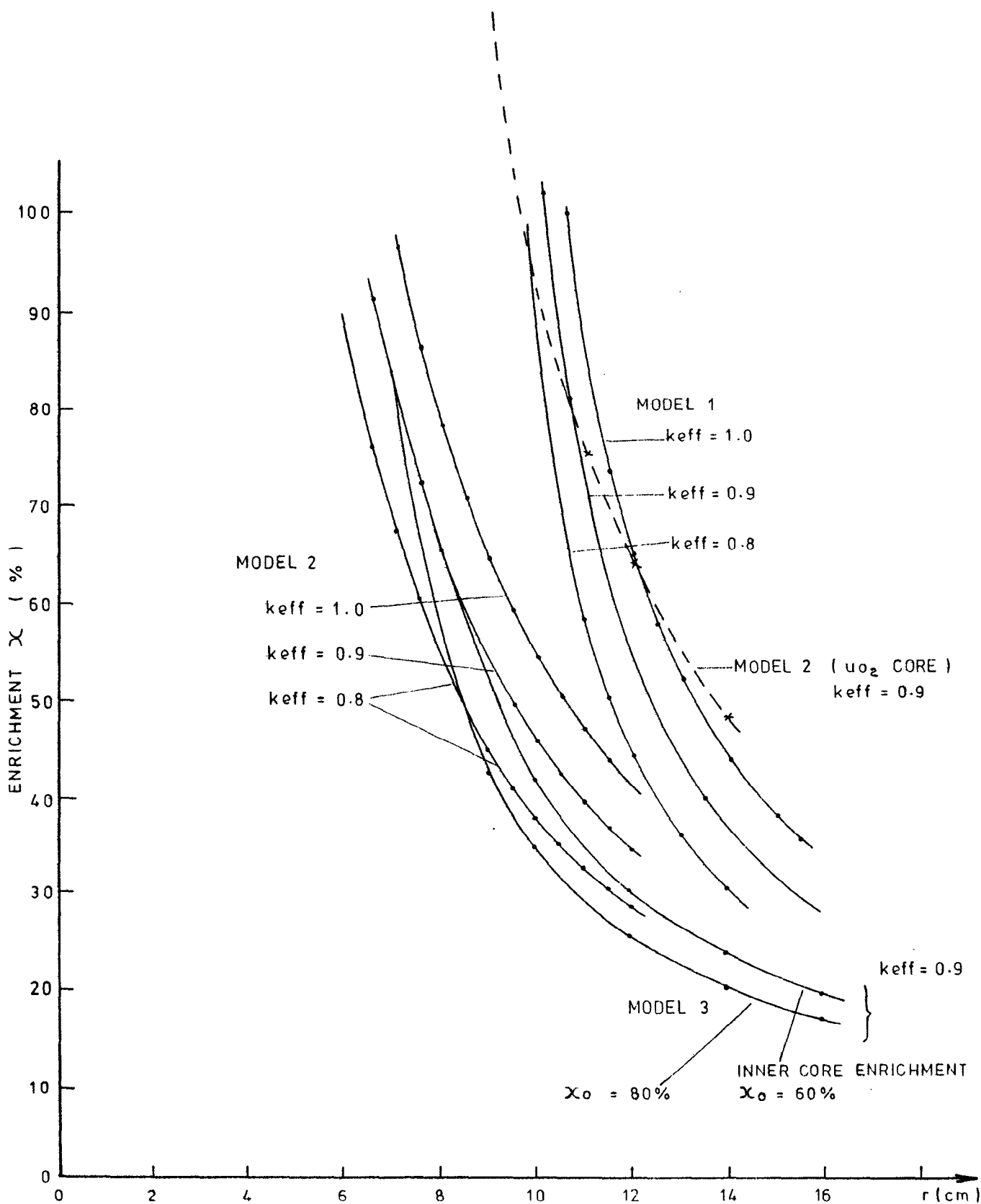


Fig. 4  
Enrichment vs core radius for Models 1-3.

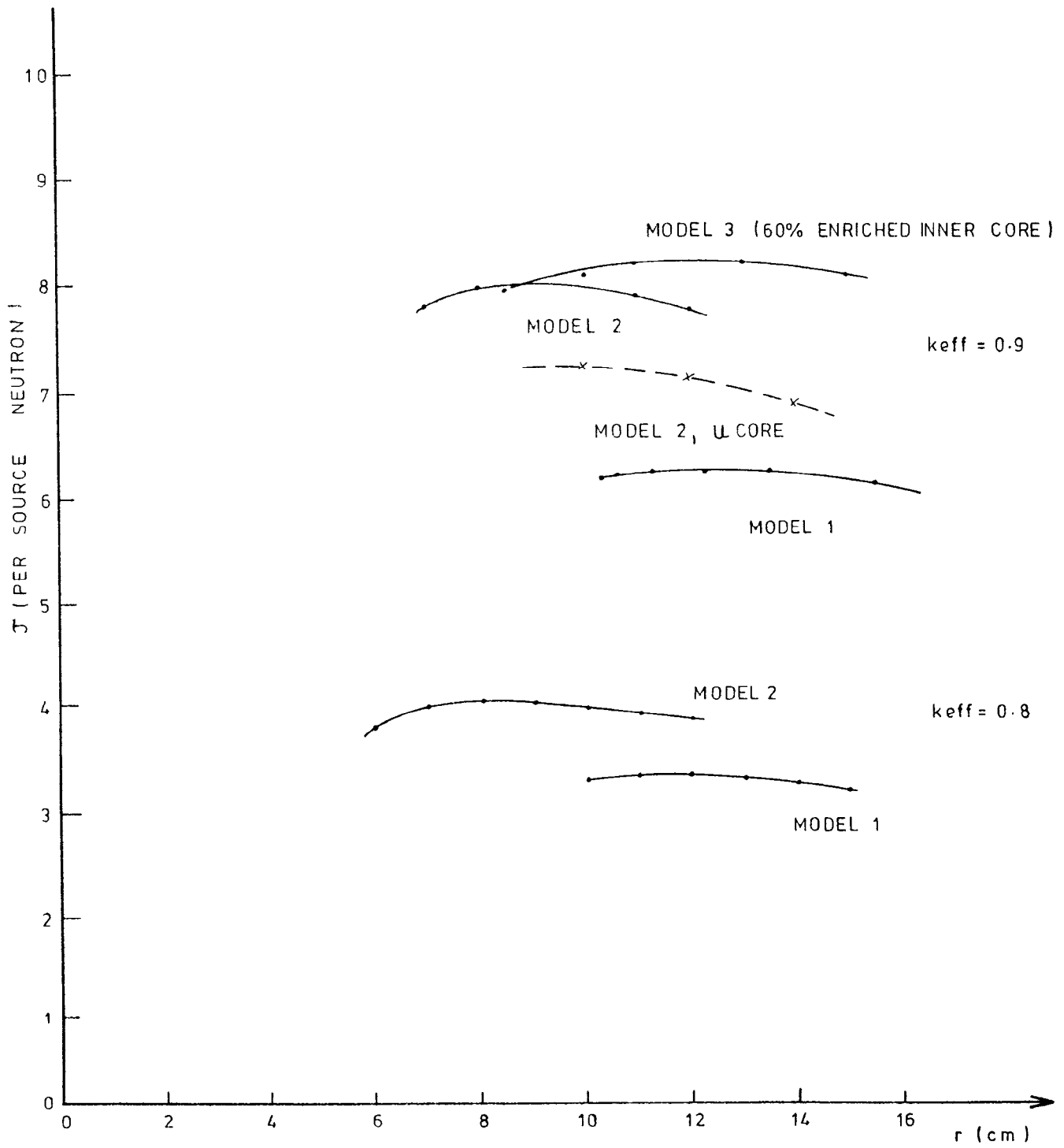


Fig. 5

Integrated net leakage  $J$  is core radius  $r$ .

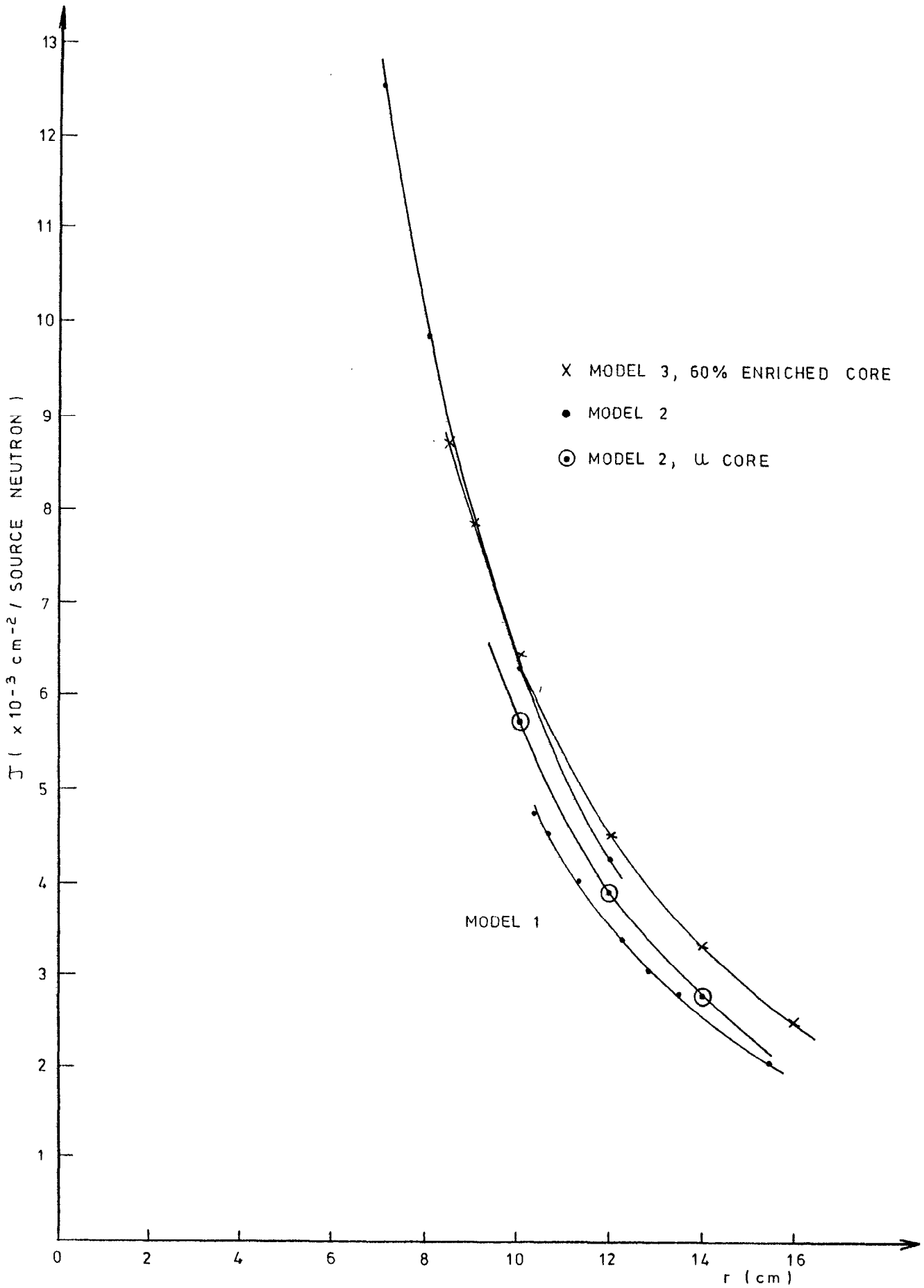


Fig. 6

Leakage per unit area for Models 1-3 ( $k_{eff} = 0.9$ )

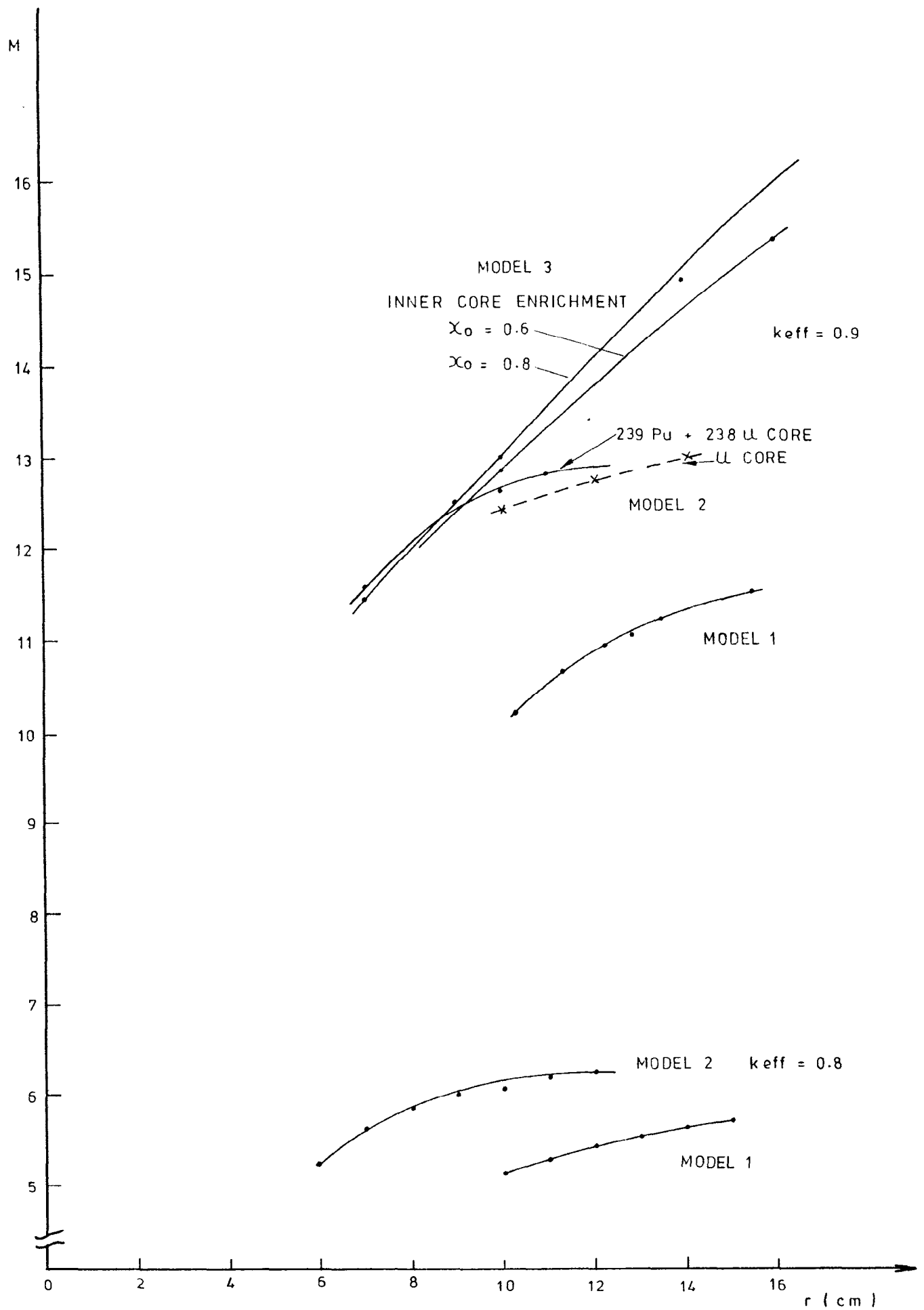


Fig 7

Total Multiplication factor M is core radius for Models 1-3.

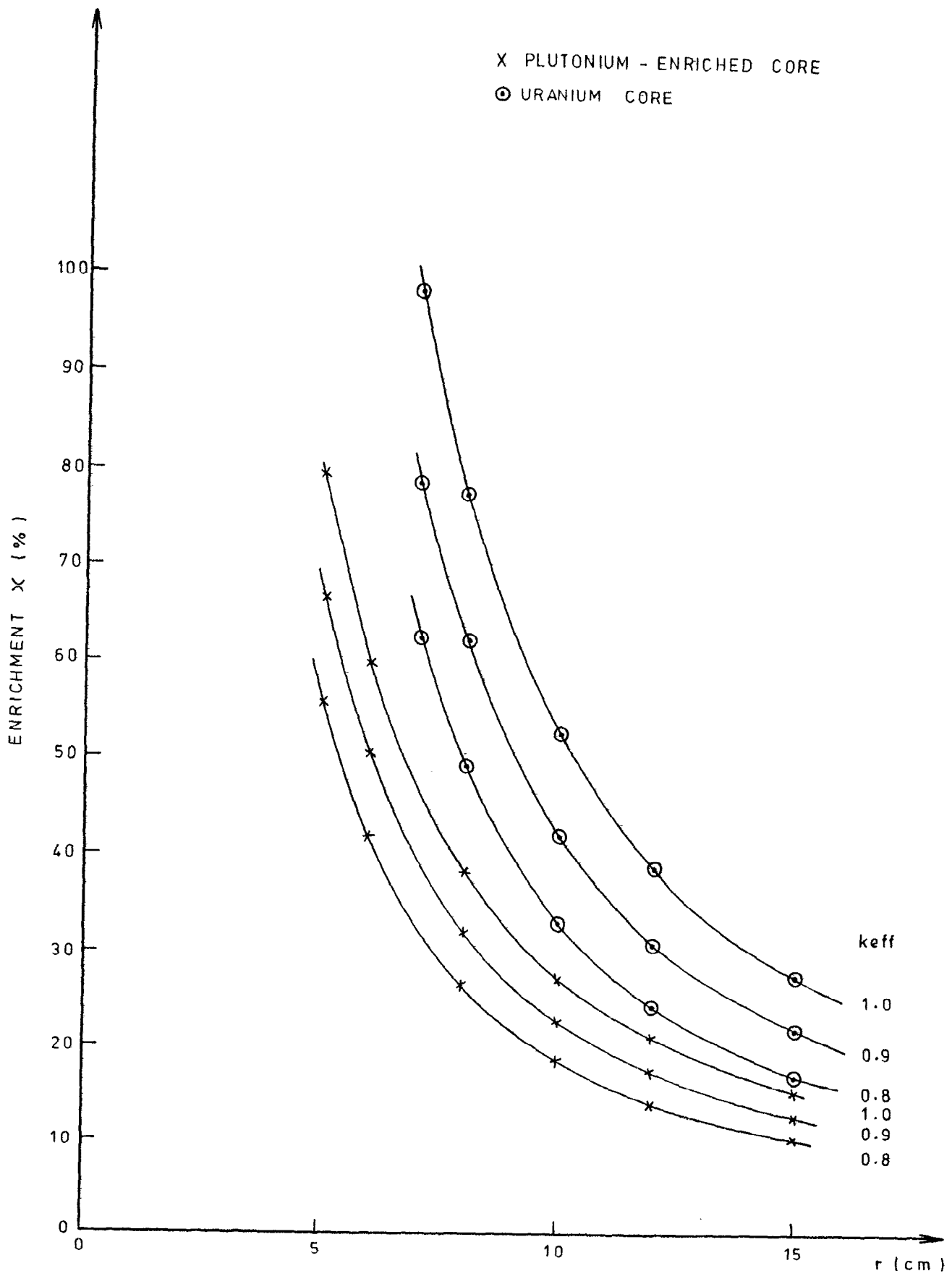


Fig. 8

Model 4: Enrichment vs radius



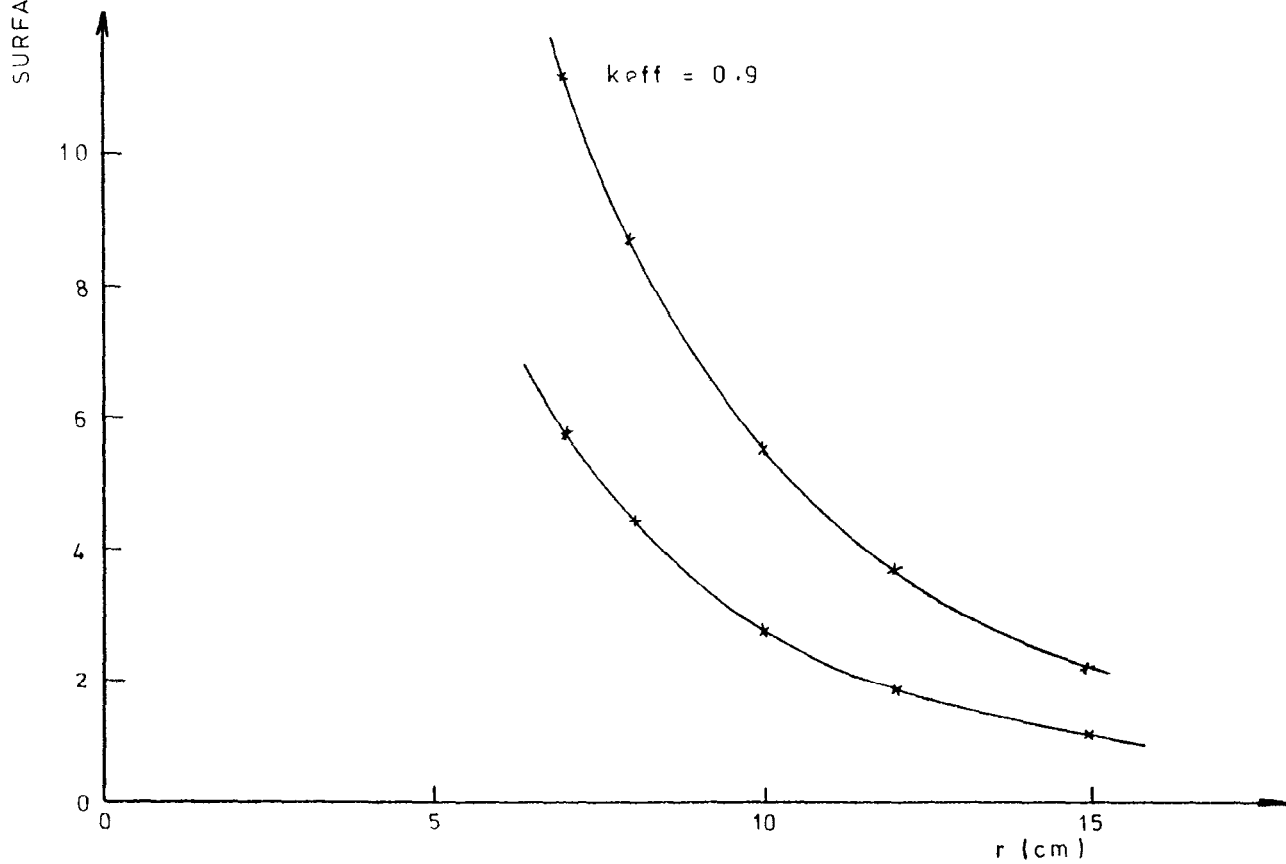
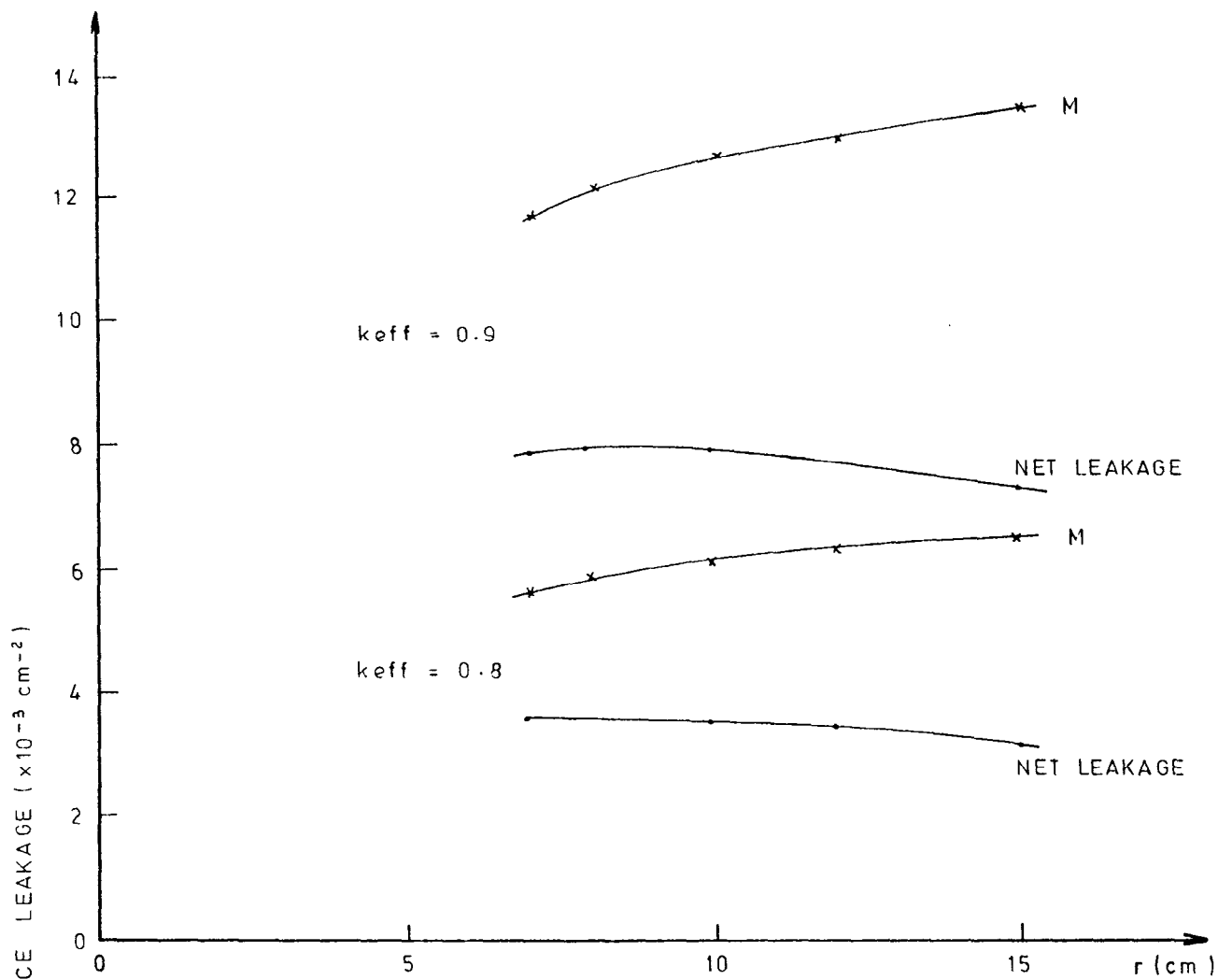


Fig. 9

Fixed source calculation: results for Model 4 (uranium system).

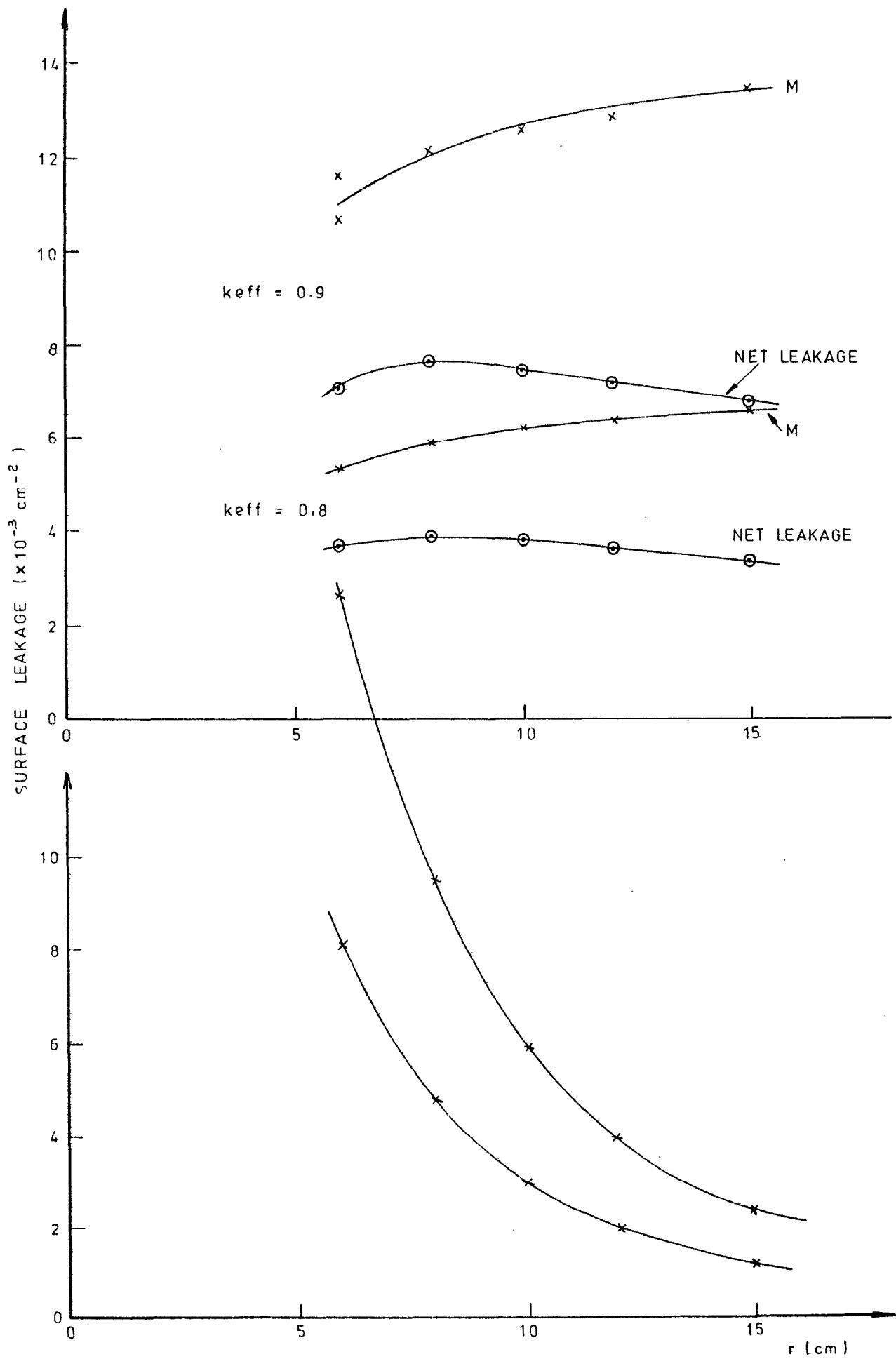


Fig. 10

Fixed source calculations: results for Model 4 ( $^{239}\text{Pu} + ^{238}\text{U}$  system).